Title

Epigenetic Regulation of Nutrient Transporters in Rheumatoid Arthritis Fibroblast-like Synoviocytes

Journal

Arthritis & Rheumatology, 74(7)

ISSN

2326-5191

Authors

Torres, Alyssa
Pedersen, Brian
Cobo, Isidoro
et al.

Publication Date

2022-07-01

DOI

10.1002/art.42077

Peer reviewed

HHS Public Access

Author manuscript

Arthritis Rheumatol. Author manuscript; available in PMC 2023 July 01.

Published in final edited form as:

Arthritis Rheumatol. 2022 July ; 74(7): 1159–1171. doi:10.1002/art.42077.

Epigenetic Regulation of Nutrient Transporters in Rheumatoid Arthritis Fibroblast-Like Synoviocytes

Alyssa Torres[1,*], **Brian Pedersen, MD**[1,*], **Isidoro Cobo, PhD**[2], **Rizi Ai, PhD**[3], **Roxana Coras, MD**[1,4], **Jessica Murillo-Saich, PhD**[1], **Gyrid Nygaard, PhD**[1], **Elsa Sanchez-Lopez, PhD**[5], **Anne Murphy, PhD**[5], **Wei Wang, PhD**[3], **Gary S Firestein, MD**[1], **Monica Guma, MD, PhD**[1,4,5]

[1]Division of Rheumatology, Allergy and Immunology and, School of Medicine, University of California, San Diego, CA 92093, USA

[2]Department of Cellular and Molecular Medicine, School of Medicine, University of California, San Diego, CA 92093, USA

[3]Department of Chemistry and Biochemistry, Department of Cellular and Molecular Medicine, University of California, San Diego, CA 92093, USA

[4]Department of Medicine, Autonomous University of Barcelona, Plaça Cívica, 08193, Bellaterra, Barcelona, Spain

[5]VA Medical Center, San Diego, California

Abstract

Objective: As previous studies indicate that metabolism is altered in rheumatoid arthritis (RA) fibroblast-like synoviocytes (FLS), we hypothesize that changes in the genome-wide chromatin and DNA states of genes associated with nutrient transporters would help to identify activated metabolic pathways in RA FLS.

Methods: Data from a previous comprehensive epigenomic study in FLS were analyzed to identify differences in the genome-wide states and gene transcription between RA and osteoarthritis (OA). Single nearest genes to regions of interest were utilized for pathway analyses. HOME's promoter analysis was used to identify enriched motifs for transcription factors. Role of SLC transporters and glutamine metabolism by RA FLS was determined by siRNA knockdown, functional assays, and incubation with CB-839, a glutaminase inhibitor. 1H-NMR was performed to quantify metabolites.

Corresponding author: Monica Guma, MD, PhD., University of California, San Diego (UCSD), 9500 Gilman Dr. MC 0663, La Jolla, CA, 92093-0663, +1 858-822 6523, mguma@health.ucsd.edu.

*these authors contributed equally as first co-authors

AUTHOR CONTRIBUTIONS

ANT, RC and JMS performed the FLS experiments, BP, RA, GN analyzed the epigenetic datasets, IC conducted the RNA-Seq experiment, JMS performed and interpreted the MRS analysis. ESL, AM, WW, GF and MG analyzed and interpreted the experiments. MG designed the project, supervised the overall project and wrote the manuscript.

Authors do not have any conflict of interest.

CONFLICTS OF INTEREST

The authors declare that the research was conducted in the absence of any commercial or financial relationships that could be construed as a potential conflict of interest.

Results: As per the unbiased pathway analysis, “SLC-mediated transmembrane transport” was one pathway associated with differences in at least 4 genome-wide states or gene transcription. 34 amino acid and other nutrients transporters were associated with a change in at least 4 epigenetic marks. Functional assays revealed that SLC4A4 was critical for invasion and that glutamine was sufficient as an alternate source of energy to glucose. Experiments with CB-839 demonstrated decreased RA FLS invasion and proliferation. Finally, enrichment of motifs for c-MYC was found in several nutrient transporters.

Conclusion: This study demonstrates that changes in the epigenetic landscape of genes related to nutrient transporters and metabolic pathways identify RA-specific targets, including critical SLC transporters, enzymes, and transcription factors, to develop novel therapeutic agents.

Introduction

Metabolomic studies show that rheumatoid arthritis (RA) is associated with metabolic disruption. (1, 2) This is likely a reflection of the increased bioenergetic and biosynthetic demands of chronic inflammation and changes to nutrient and oxygen availability in tissues during inflammation. The synovial membrane lining layer is the principal site of inflammation in RA. (3) Here, fibroblast-like synoviocytes (FLS) are transformed toward overproduction of enzymes which degrade cartilage and bone, and cytokines which promote immune cell infiltration. (4, 5) Prior studies from our group and others have shown several metabolic changes in FLS from RA patients and these may be therapeutically targetable. (6–9) These metabolic changes could be targeted without compromising systemic homeostasis as a novel approach for combination therapy independent of systemic immunosuppression.

Recent studies in cancer or other activated cells reveal similar metabolic changes. (10) These changes often involve increased expression of nutrient transporters to supplement the elevated needs of the activated cell. (11) Nutrient transporters, with the solute carrier (SLC) transporter families that contain approximately 400 genes and 52 subfamilies among others, serve as ‘metabolic gates’ for cells by mediating the transport of several different nutrients and metabolites such as glucose, amino acids, vitamins, neurotransmitters, and inorganic/metal ions. (12) For instance, an elevated level of glutamine transporters that correlate with an increase of glutamine metabolism is observed in activated cells in cancer (13) and other diseases including neurodegenerative diseases (14) and arthritis. (15) In response to these metabolic alterations, glutamine can be relied on to ultimately assist in the TCA cycle as an alternative carbon source to glucose. Other groups have recently described SLC transporter effects in arthritis in other nutrients besides glutamine in both FLS and lymphocytes. (16, 17) Other investigations of non-amino acid transporter roles in cancer are looking at mitochondrial carriers, (18) zinc transporters, (19) and bicarbonate transporters, (20) to name a few.

Epigenetic alterations such as DNA methylation and histone modification might contribute to disease pathogenesis by enhancing chromatin accessibility to activate genes coding for these nutrient transporters. (21, 22) Of interest, several studies have described epigenetic changes (DNA methylation, histone modification and microRNA expression) in FLS. (23, 24) A comprehensive epigenomic characterization of RA FLS was recently described. (25)

As previous studies indicate that metabolism is altered in RA FLS, we hypothesize that changes in the histone landscape of genes associated to nutrient transporters would correlate with differences in expression and this would help identify activated metabolic pathways and thus targets for RA pathogenesis. Therefore, studying epigenetic changes in nutrient transporters may not only highlight important metabolic pathways, but it could also lead us to specific nutrients and transporters essential to creating a metabolic shift in inflamed tissue. Targeting these specific nutrients and pathways could result in an insufficient energy supply and thus reduce the aggressive FLS phenotype involved in the pathogenesis of RA.

Materials and methods

Genome-wide datasets:

A total of 191 genome-wide datasets were generated across 11 RA and 11 OA samples and characterized in our previous work, (25) and was deposited in Gene Expression Omnibus with the primary accession code GSE112658. Briefly, it includes 130 histone modification datasets, 22 open chromatin datasets, 20 RNA-seq datasets and 19 DNA methylation datasets. Six histone modification marks were analyzed, including histone H3 lysine 4 trimethylation (H3K4me3), associated with promoter regions; H3 lysine 4 monomethylation (H3K4me1), associated with enhancer regions; H3 lysine 27 acetylation (H3K27ac), associated with increased activation of promoter and enhancer regions; H3 lysine 36 trimethylation (H3K36me3), associated with transcribed regions; H3 lysine 27 trimethylation (H3K27me3), associated with Polycomb repression; and H3 lysine 9 trimethylation (H3K9me3), associated with heterochromatin regions. Additional epigenomic marks include open chromatin regions, profiled by ATAC-Seq, denoting regions of accessible chromatin, and typically associated with regulator binding; DNA methylation, commonly associated with repressed regulatory regions, profiled with whole-genome bisulfite sequencing (WGBS); and RNA-Seq used for measuring gene expression levels. Images were generated using Integrative Genomics Viewer version 2.3.98. Epigenetic analysis of the nutrient transporters was conducted as described in (25).

Human FLS:

FLS were extracted from patients with RA or OA undergoing total joint replacement as previously described. (26) RA and OA FLS were grown in Dulbecco's Modified Eagle Medium (DMEM) without sodium pyruvate supplemented with 10% Fetal Bovine Serum (FBS), 2 mM L-glutamine, and 100 units/ml penicillin and 100 ug/ml streptomycin. Experiments testing glucose and glutamine concentrations were done with DMEM lacking glucose, glutamine, phenol red, and sodium pyruvate (Gibco, #A1443001) with dialyzed FBS (Gibco, #A3382001). In experiments testing the lack of various amino acids without glucose, we used DMEM with no glucose, sodium pyruvate, phenol red, lysine, and arginine (Gibco, #A24939-01) and dialyzed FBS.

RNA-Seq:

4 RA FLS cell lines and 3 OA FLS cell lines were plated using 100,000 cells per well in a 6-well plate, starved overnight in 1% dialyzed serum and stimulated with either 2mM or

25mM glucose in 6mM glutamine for 5 hours. RNA-Seq was performed and analyzed as described elsewhere, (27–29) and in supplementary methods.

Gene Set Enrichment Analysis (GSEA):

Analysis of signalling pathways regulated by differentially expressed genes was performed with the Molecular Signature Database (MSigDB) of GSEA (30–32) computing the overlaps with PID, Reactome, Wikipathways, Hallmark or KEGG datasets as indicated in the Figure legends and Supplementary Files.

Nuclear Magnetic Resonance (1H-NMR) experiments:

Approximately 600,000 RA FLS were starved for 4 hours of glutamine and glucose, and then incubated with either DMSO or CB-839 (300nM) with 10 ng/ml PDGF for 4 hours in media with 6mM glutamine and without glucose for metabolite extraction as described elsewhere, (33–35) and in supplementary methods.

NMR Acquisition and Processing:

NMR spectra were recorded using a 600 MHz Bruker Avance III NMR spectrometer fitted with a 1.7mm triple resonance cryoprobe. The standard Bruker pulse sequence “noesygppr1d” was used with a mixing time of 500 ms. A daily quality assurance procedure was performed before sample data acquisition, involving temperature checks and calibration as well as shim and water suppression quality. The data acquisition was obtained in the NMR facility of Skaggs School of Pharmacy and Pharmaceutical Science, University of California San Diego.

Metabolites Identification and Quantification:

The identification of metabolites was performed using the software Chenomx NMR suite 8.5 professional (Chenomx Inc., Edmonton, Canada) 600 mHz, version 11 which contains a library in the profile to match peaks of compound according to the chemical shift. Metabolite concentrations were normalized according to the TSP-d4. Cell pellet were normalized according to protein quantification through Bradford. Supernatants concentrations are provided after subtraction from media control, and a negative value suggests that the metabolite has been consumed by cells in culture. The metabolite concentrations were reported in micromolar (μM).

Statistical analysis:

Statistical analysis was performed with Prism software (version 8; GraphPad). Results are expressed as the mean ± standard deviation (SD). Normality of the variables was assessed using the Kolmogorov-Smirnov normality test or the Shapiro-Wilk normality test. For comparison between more than two conditions, ordinary one-way ANOVA or Kruskal-Wallis tests were used depending on normality of the distribution of the variables followed by Tukey’s or Dunn’s multiple comparisons test, respectively. Results were considered significant if the 2-sided p-value was less than 0.05. Heat maps performed with R software show Pearson’s correlation coefficients for gene expression. Color keys are labeled above heat map and shows the strength and direction of the correlation. Correlation ranges from −1

to +1. The greater R-square the better the model. We considered weak correlation if Pearson Correlation coefficient was between −0.3 to −0.5 or 0.3 to 0.5, moderate correlation between −0.5 to −0.7 and 0.5 to 0.7, and strong correlation between <−0.7 and >0.7. Our sample size of 10 RA and 10 OA FLS can detect a Pearson's correlation coefficient of r =0.7 with 80% power (alpha =0.05, two-tailed).

More detailed methods are provided as supplementary methods

Results

Unsupervised analysis of Metabolic Pathways Associated with Differential Marking between OA and RA FLS.

Histone modifications, WGBS, ATAC-Seq and RNA-Seq data were analyzed individually to identify metabolic pathways associated with differential genome-wide chromatin and DNA states, and gene expression between OA and RA FLS. Interestingly, together with the significant enrichment of pathways involved in inflammation, immune response, matrix regulation, and cell migration, listed in Supplementary File 1, we identified several enriched metabolic-related pathways in RA FLS. Figure 1A shows the metabolic-related pathways and number of occurrences, and Figure 1B shows the pathways per histone modification, WGBS, ATAC-Seq and RNA-Seq. Interestingly, enriched metabolic pathways were only associated with changes in activating histone marks linked to increased expression of the downstream genes such as H3K4me1, H3K4me3 and H3K27ac, but not in repressive histone marks such as H3K9me3, H3K27me3 or H3K36me3. Pathways associated with more than 5 differentially modified genome-wide chromatin and DNA states between OA and RA FLS included PI3K-Akt signaling and metabolism of carbohydrates. PI3K-Akt signaling is a well-known pathway involved in metabolic reprogramming and metabolism of carbohydrates and previously described to play an important role in the FLS aggressive phenotype by our groups and others. (36–40) The pathway "solute carrier (SLC)-mediated transmembrane transport" is another pathway that stood out to us as significant. These data indicate that alterations in chromatin accessibility and activation of regulatory regions associated with metabolic genes is a feature of FLS in RA.

SLC-mediated transmembrane transporters showed differential marking between OA and RA FLS.

Our epigenetic analyses suggest a role for SLC transporters in RA FLS. We decided to conduct a supervised analysis of the epigenetic changes in genes from the SLC transporter families. The histone modifications, WGBS, ATAC-Seq, and RNA-Seq data corresponding to approximately 350 genomically encoded genes of the SLC transporter family were probed for differences between RA and OA (Supplementary File 2). Of these SLC genes, 78 were associated with at least 3 differentially modified genome-wide chromatin and DNA states between OA and RA FLS, and 32 genes were associated with at least 4 (Supplementary File 2). Pathway analysis with these 78 genes was performed to identify predominant nutrient transporters is shown in Figure 2A. Other than hexose transport (which includes glucose and fructose), the more significant transporters were classified as amino acids transporters.

The chart in Figure 2B details the genes with greater than 4 differentially modified marks comparing RA and OA FLS. H3K27ac and H3K4me1 were the most commonly differentially changed histone modifications and correlated with significant changes in ATAC-Seq. As shown in Figure 2B, these transporters were mostly related to amino acid transporters, including glutamine transporters (SLC38A1, SLC38A4, SLC7A11, SLC7A5, SLC7A8, SLC1A4). Other transporters that were differentially regulated between OA and RA were ions transporters including zinc and bicarbonate transporters, such as SLC4A4, a bicarbonate transporter that is heavily differentially regulated between OA and RA FLS (Figure 2B), and for which expression is comparatively higher in OA FLS (Figure 2C). Of note, siRNA knockdown of the *SLC4A4* resulted in an increase of invasion but not migration compared to the control siRNA, suggesting that this transporter is repressed in RA FLS to increase its aggressive phenotype. (Figure 2D and Supplementary Figure 1A). Supplementary Figure 1B is a depiction of significant SLC transporter genes that have greater than 4 differentially modified marks comparing RA and OA FLS and their location in the cell.

We also performed correlations between the expression of the nutrient transporters more differentially marked between 10 RA and 10 OA FLS cell lines, and the expression of various genes related to FLS relevant functions including synovial fluid molecules (*PRG4 and HAS1*), metalloproteinases (*MMP1, MMP3*), *IL-6*, chemokines (*CXCL1, CCL2*), genes involved in cell invasion and migration (*POSTN, PLOD2, ACTA2, PDGF*) and angiogenesis (*VEGF, FGF2*), and genes involved in fibrosis (*PLOD2, COL1A1*). (4–6, 36, 41–44) Figure 2E and Supplementary Figure 1C shows the association between amino acid-related SLC transporters (Figure 2E) or other nutrient-related SLC transporters (Supplementary Figure 1C). Several SLC transporters showed moderate or strong correlation with these genes in both OA and RA FLS, for instance between *SLC15A4* and *IL-6*, suggesting a critical role of this transporter in IL-6 expression in all synovial fibroblasts. Of interest, two transporters, *SLC38A1* (a transporter of glutamine) and *SLC15A1* (transports the dipeptide L-alanyl-L-glutamine) moderately or strongly correlated (correlation coefficient, r, more than 0.5) with more than one of these genes, including chemokines (*CXCL1, CCL2*), metalloproteinases (*MMP1*), and genes involved in cell invasion in RA FLS (*POSTN, PLOD2* and *PDGFC*) in RA FLS. The expression of SLC39 transporters, which controls the influx of zinc into the cytoplasm, but not SLC30 transporters, which controls the efflux of zinc, moderately or strongly correlated with these genes in RA but not in OA FLS (Supplementary Figure 1C). In OA FLS, other SLC transporters moderately or strongly correlated with more than one of these genes including *SLC15A4* (histidine carrier), and *SLC7A1* (alanine, serine, cysteine, and threonine transporter). As recent evidence emphasizes the emergent role of FLS-mediated synovitis in OA, (45) these differential correlations in RA and OA FLS suggest different key FLS transporters in both diseases.

Glutamine availability enhances invasion, migration and proliferation but not cytokine secretion in RA FLS

Among other nutrients, some of the more significant heavily differentially regulated SLC transporters between OA and RA FLS were related to amino acid transporters (Figure 2B), specifically glutamine transporter (SLC38A1, SLC38A4, SLC7A11, SLC7A5, SLC7A8,

SLC1A4), we tested whether glutamine metabolism was important for the FLS aggressive phenotype. We first determined glutamine uptake by measuring intracellular levels after glucose starvation and with or without additional PDGF stimulation. As shown in Figure 3A, intracellular glutamine increased after PDGF stimulation in RA FLS.

We then tested whether an increase of glutamine availability would enhance the invasive phenotype of RA FLS. As shown in Figure 3B and C, an increase of the amount of glutamine in the media increased the RA FLS invasiveness under glucose deprivation. These results were not observed when RA FLS were treated with different concentrations of arginine or lysine (Supplementary Figure 2A). Of interest, when comparing either glucose or glutamine in the media, RA FLS efficiently used either carbon sources during its invasion (Figure 3D). In addition, migration was also dependent on glutamine in RA FLS (Figure 3E). Of note, OA FLS had a more heterogenous glutamine dependence during migration (Supplementary Figure 2B).

In Figure 4A–C, viability measured by MTT assay and proliferation measured by EdU assay showed glutamine dependence in the absence of glucose in RA FLS. As with the migration, RA FLS were found to also use glutamine in the absence of glucose for proliferation (Figure 4D). OA FLS showed similar behavior that RA FLS in proliferation (Supplementary Figure 2C). Of note, MMP3, IL6, and CCL2 secretion after PDGF and TNF stimulation were not glutamine dependent (Supplementary Figure 3A,B). Yet, siRNA knockdown of *SLC38A1*, one of the glutamine transporters that was heavily differentially marked between OA and RA, and for which expression was significantly upregulated in RA compared to OA FLS, did not decrease the invasion or migration. This suggests some redundancy in the glutamine transporters (Supplementary Figure 3C–E).

Glutamine pathways related enzymes showed differential marking between OA and RA FLS

Since targeting an enzyme might be a more feasible approach to inhibit the glutamine metabolic pathway than targeting several transporters involved in glutamine transport, we analyzed the enzymes related to the glutamine pathway. The different histone marks, RNA-Seq, ATAC-Seq and WGBS dataset with a change in signal in the RA vs. OA samples were analyzed in a list of 19 genomically encoded genes of glutamine related enzymes (Supplementary File 3). Given that glucose metabolism was associated with the FLS aggressive phenotype (38–40) and glucose transporters were also differentially marked between RA and OA FLS, we also analyzed 83 generically encoded genes related to glucose metabolism (Supplementary File 3). Figure 5A and Supplementary Figure 4A details the type of dynamic chromatin changes for each of the listed histone post-translational modifications, ATAC-Seq, RNA-Seq and WGBS signal of the genes associated with at least 4 differentially modified genome-wide chromatin and DNA states in RA FLS compared to OA FLS. Several glucose metabolism related genes were heavily differentially marked and correlated with significant changes in ATAC-Seq, including PCK2, PDHB, PGM1. Of interest HK2, a glycolytic enzyme recently described as a key gene in regulating the aggressive phenotype in RA FLS, (26, 46) was also heavily differentially marked. HK2 was also the gene that moderate or strongly correlated with genes related to RA FLS aggressive

phenotype (Supplementary Figure 4B). Our epigenetic analysis also found GLS, GOT2 and GFPT2 as the glutamine metabolism related enzymes that were more differentially marked between RA and OA FLS. GLS and GOT2 seemed to be more critical in RA FLS and GFPT2 in OA FLS (Figure 5B).

Glutaminase, a key target for FLS aggressive phenotype

Glutaminase (GLS), which is responsible for the conversion of glutamine to glutamate, plays a vital role in upregulating cell metabolism for tumor cell growth and is considered to be a valuable therapeutic target for cancer treatment. Several GLS inhibitors have been developed and are currently being evaluated in phase 1 and 2 clinical trials. Thus, we focused on GLS to determine whether GLS could be a feasible target for the FLS aggressive phenotype. In Figure 5C, we show that GLS is expressed in both the lining and sublining of RA synovial tissue. We then looked at the effect of CB-839 compound, an inhibitor of glutaminase (GLS), on FLS metabolism, proliferation, and invasion. We first analyzed the metabolic effect of CB-839 after PDGF stimulation. Supplementary Figure 5A shows the effect of the inhibitor on glutamine levels. As expected, there was a significant increase of intracellular glutamine in the presence of the inhibitor. Interestingly, other intracellular nutrients including choline, isoleucine, glycine, and threonine were also more significant with CB-839 (Figure 5D and Supplementary Figure 5B,C). Results from MTT viability assays revealed CB-839 was non-toxic at a wide range of concentrations (Supplementary Figure 5D) and that CB-839 (300nM) was sufficient to significantly reduce the RA FLS invasion (Figure 5E) and proliferation (Figure 5F,G) but only under glucose free conditions (Figure 5E and Supplementary Figure 5E).

c-Myc, a key transcription factor for FLS aggressive phenotype

To determine the regulation of the nutrition transporters in RA FLS, we performed motif enrichment analysis of the promoters of the SLC genes exhibiting differential ATAC-Seq signal between RA FLS and OA FLS (Supplementary Figure 6A). In addition, we performed analysis of the motifs of the promoter regions of genes that displayed differentially modifications in at least four genome-wide chromatin and DNA states and found enrichment of motifs for c-MYC and the nuclear receptors TLX, RORa and RORg, (Figure 6A). Supplementary Figure 6B shows the number of putative c-Myc binding sites in the SLC transporters analyzed. Some of the SLC, including transporters involved in lactate/pyruvate (SLC16A3 and SLC16A6), zinc (SLC39A10), and amino acids (SLC38A1 and SLC7A8) had a high number of putative binding sites. Importantly, c-Myc was expressed in the lining of RA tissues (Figure 6B), and its inhibition in FLS altered the intracellular levels of pyruvate and several amino acids, including glutamine, , pyruvate, succinate, alanine, and valine suggesting changes in their transport and/or its metabolic pathways (Figure 6C and Supplementary Figure 6C).

Since c-Myc is known to regulate the expression of genes especially under glucose starvation (47), and RA FLS kept its aggressive phenotype even under glucose deprivation, we wondered whether c-Myc was also involved in the regulation of RA FLS phenotype under this condition. We performed RNA sequencing of 4 RA FLS and 3 OA FLS cell lines incubated with 25mM or 2mM of glucose for 5h. to address which signaling pathways

are deregulated upon glucose deprivation. Differential expression analysis showed 225 upregulated genes in RA 2mM vs. OA 2mM, 138 unregulated genes in RA 25mM vs. OA 25mM, 167 downregulated genes in RA 2mM vs. OA 2mM, and 168 downregulated genes in RA 25mM vs. OA 25mM (Figure 6D). Gene set enrichment analysis (GSEA) of differentially expressed genes between RA 25mM vs. OA 25mM or RA 2 mM vs. OA 2 mM showed activation of MYC targets and PI3K-AKT signaling, that were only differently activated in RA FLS 2 mM vs. OA FLS 2mM (Figure 6E). These results suggest that MYC and PI3K-AKT pathways are involved in the distinct response of RA FLS to starving levels of glucose. Upon investigation of the effect of a c-Myc inhibitor on RA FLS at a viable dosage (Supplementary Fig 6D), c-Myc inhibition attenuated RA FLS migration and invasion (Figure 6F,G). Of note, c-Myc inhibitor was able to significantly attenuate RA FLS migration only when cultured in 2mM of glucose and not in 25mM of glucose, but interestingly was equally attenuated in RA FLS invasion.

DISCUSSION

The epigenetic alterations of metabolic genes in OA vs. RA FLS are largely unknown. Here, we describe the epigenetic changes in metabolic genes related to SLC-transporters between RA and OA FLS. This might help to better understand the increased demand for nutrients in the RA synovial. (1) For instance, when glucose demand is high in the RA synovium, the upregulation of glutamine transporters may allow FLS to utilize other sources for energy. Our results showed that glutamine served as an alternate carbon source in the absence of glucose. In addition, RA FLS did not utilize other amino acids such as lysine and arginine. Even though FLS seemed to uptake other amino acids and nutrients during GLS inhibition, they did not have a role on invasion or proliferation. Of interest, OA FLS also utilized glutamine, although we were unable to detect large differences in *in vitro* glutamine metabolism between OA and RA FLS in these conditions. This could indicate that either the overall differences in glutamine metabolism between OA and RA FLS are subtle in cell culture, or we could not mimic the *in vivo* inflamed synovial conditions in which RA FLS would show greater glutamine metabolic changes than OA FLS.

Our results also suggest that inhibiting glutamine metabolism through a GLS inhibitor (CB-839) could potentially suppress aggressive features of RA FLS, such as invasion, migration, and proliferation. (48) Even though the differences with OA are small, the important role of glutamine in those functions suggest that they could be important in the context of rheumatoid synovitis. Glutamine metabolism has also been a focus in recent years for other diseases such as cancer, (49, 50) and clinical trials using glutaminase inhibitors are underway in cancer research. (50) Since glutamine metabolism seems not to play a role in cytokine secretion, the inhibition of glutamine metabolism would mostly target the FLS aggressive phenotype and could complement current immunotherapies. In addition, inhibiting the GLS enzyme could prove more effective than knockdown of certain SLC glutamine transporters, since they may have a redundant function.

Future studies are needed to investigate more in depth the role of glutamine and other amino acid transporters (such as SLC7A11) in order to inhibit its aggressive phenotype and to promote only essential homeostatic FLS functions. Tracing experiments and not just

paired supernatant-pellet concentrations are needed to better determine changes of amino acid levels and the role of these amino acid transporters. Of note, SLC transporters have long been used as a drug target in RA as sulfasalazine is a non-specific inhibitor of SLC7A11, which facilitates the import and export of the amino acid glutamate and cystine.

Other nutrient transporters are potential therapeutic targets. Our epigenetic analysis could help prioritize the transporters and target specific activated metabolic pathways in synovial RA. For example, many other transporters specific to choline, ions like zinc, sodium, and calcium, as well as bicarbonate, nucleosides, lactate and mitochondrial carriers are differentially regulated between RA and OA. A prior study from our group described a role of choline in RA FLS phenotype. (51) Our analysis points at SLC22A3 and SLC44A3 as potential key choline transporters in FLS. The role of zinc in FLS RA was also recently described. (52) SLC39A10 and SLC39A11 could be promising candidates for targeted inhibition of zinc transport. Although the correlation analysis could highlight specific FLS transporters in both OA and RA cell lines, results need to be interpreted with caution given the limited power of the analysis and the need for additional biologic validation.

Our study also suggests a possible role for bicarbonate transporters, mitochondrial carriers, and nucleosides for RA pathogenesis and might also serve as attractive transporter targets in RA. Bicarbonate transporters have large roles in regulating pH in cancer through the SLC4 family of transporters. (20) The role of these transporters seems to have different purposes which need more exploration. For example, *SLC4A4* is upregulated in breast cancer cells and its knockdown reduces migration (20). Yet, in FLS, *SLC4A4* transporter is higher in OA as compared with RA and its downregulation further increases the invasive phenotype but not migration of RA FLS. Of note, migration across a surface and invasion into extracellular matrix are distinct biological functions and involve distinct patterns of gene expression, such as proteases, to degrade the matrix at the leading edge. The SLC25 family is comprised of mitochondrial carriers and have been found to be biomarkers in cancers and regulate several different types of substrates like amino acids, nucleotides, carboxylates, and keto acids. (18) Nucleosides can be used as precursors to essential molecules like ATP but can also be used as signaling molecules. (53) Yet, no information on the role of these transporters in RA FLS has been described so far. Future studies can look into the specific role of other SLC transporters in RA FLS, and will determine whether the specific transporter, a key enzyme, or a transcription factor is the most feasible option to regulate that metabolic pathway.

Other than specific transporters, one metabolic regulator, c-Myc, which plays an important role in cancer metabolism, (54) appeared in our analysis suggesting a role of this transcription factor in metabolic reprograming of RA FLS. C-Myc promotes glutamine usage by upregulating GLS and in addition upregulates GOT2 and glutamine synthetase, which allow for dependence on glutamine in cancer by turning glutamate back into glutamine. (47) Lactic acid and pyruvate can also be regulated by c-Myc. (55) SLC16A3, another transporter identified in our analysis, transports lactate and pyruvate. Interestingly, Ras- and c-Myc-dependent signaling events cooperated to regulate the growth and invasiveness of RA FLS. (56) Further experiments are needed to understand the role of c-Myc under stress conditions, such as starvation and hypoxia, on glutamine metabolism and how it might contribute to RA pathogenesis. In addition, while specific targets of c-Myc

have been challenging to create due to its structure and location, the identification of new binding partners such as BPTF, (57) and other new strategies to inhibit c-Myc have been recently described. (58)

Overall, RA FLS demonstrate changes in epigenetic marks associated with genes related to metabolism and nutrient transporters. Validation studies of one pathway demonstrated that the glutamine pathway, and specifically glutaminase inhibition, could regulate the aggressive phenotype of RA FLS. Additionally, this dataset has the potential to identify other RA targets that can be used to develop novel therapeutic agents.

Supplementary Material

Refer to Web version on PubMed Central for supplementary material.

FUNDING

This work was supported by the National Institutes of Health (R01AR073324 to MG, NIH Diversity Supplement to AT, T32AR064194 to J.D.M.-S and RC, K01AR077111 to ESL, P30AR073761 to GF and WW, NS087611 to AM, NS047101 to UCSD Microscopy Core), and by EMBO Long Term Fellowship (ALTF-960-2018) to IC. The content is solely the responsibility of the authors and does not necessarily represent the official views of the National Institutes of Health.

REFERENCES

1. Falconer J, Murphy AN, Young SP, Clark AR, Tiziani S, Guma M, et al. Review: Synovial Cell Metabolism and Chronic Inflammation in Rheumatoid Arthritis. Arthritis Rheumatol. 2018;70(7):984–99. [PubMed: 29579371]
2. Weyand CM, Goronzy JJ. Immunometabolism in the development of rheumatoid arthritis. Immunol Rev. 2020;294(1):177–87. [PubMed: 31984519]
3. Henderson B, Bitensky L, Chayen J. Glycolytic activity in human synovial lining cells in rheumatoid arthritis. Ann Rheum Dis. 1979;38(1):63–7. [PubMed: 434949]
4. Nygaard G, Firestein GS. Restoring synovial homeostasis in rheumatoid arthritis by targeting fibroblast-like synoviocytes. Nat Rev Rheumatol. 2020;16(6):316–33. [PubMed: 32393826]
5. Bottini N, Firestein GS. Duality of fibroblast-like synoviocytes in RA: passive responders and imprinted aggressors. Nat Rev Rheumatol. 2013;9(1):24–33. [PubMed: 23147896]
6. Bustamante MF, Garcia-Carbonell R, Whisenant KD, Guma M. Fibroblast-like synoviocyte metabolism in the pathogenesis of rheumatoid arthritis. Arthritis Res Ther. 2017;19(1):110. [PubMed: 28569176]
7. de Oliveira PG, Farinon M, Sanchez-Lopez E, Miyamoto S, Guma M. Fibroblast-Like Synoviocytes Glucose Metabolism as a Therapeutic Target in Rheumatoid Arthritis. Front Immunol. 2019;10:1743. [PubMed: 31428089]
8. Sanchez-Lopez E, Cheng A, Guma M. Can Metabolic Pathways Be Therapeutic Targets in Rheumatoid Arthritis? J Clin Med. 2019;8(5).
9. Fearon U, Hanlon MM, Wade SM, Fletcher JM. Altered metabolic pathways regulate synovial inflammation in rheumatoid arthritis. Clin Exp Immunol. 2019;197(2):170–80. [PubMed: 30357805]
10. Cairns RA, Harris IS, Mak TW. Regulation of cancer cell metabolism. Nat Rev Cancer. 2011;11(2):85–95. [PubMed: 21258394]
11. Zhu J, Thompson CB. Metabolic regulation of cell growth and proliferation. Nat Rev Mol Cell Biol. 2019;20(7):436–50. [PubMed: 30976106]
12. Zhang Y, Zhang Y, Sun K, Meng Z, Chen L. The SLC transporter in nutrient and metabolic sensing, regulation, and drug development. J Mol Cell Biol. 2019;11(1):1–13. [PubMed: 30239845]

13. Cluntun AA, Lukey MJ, Cerione RA, Locasale JW. Glutamine Metabolism in Cancer: Understanding the Heterogeneity. Trends Cancer. 2017;3(3):169–80. [PubMed: 28393116]
14. Yamada D, Kawabe K, Tosa I, Tsukamoto S, Nakazato R, Kou M, et al. Inhibition of the glutamine transporter SNAT1 confers neuroprotection in mice by modulating the mTOR-autophagy system. Commun Biol. 2019;2:346. [PubMed: 31552299]
15. Raposo B, Vaartjes D, Ahlqvist E, Nandakumar KS, Holmdahl R. System A amino acid transporters regulate glutamine uptake and attenuate antibody-mediated arthritis. Immunology. 2015;146(4):607–17. [PubMed: 26346312]
16. Xu J, Jiang C, Cai Y, Guo Y, Wang X, Zhang J, et al. Intervening upregulated SLC7A5 could mitigate inflammatory mediator by mTOR-P70S6K signal in rheumatoid arthritis synoviocytes. Arthritis Res Ther. 2020;22(1):200. [PubMed: 32867828]
17. Pucino V, Certo M, Bulusu V, Cucchi D, Goldmann K, Pontarini E, et al. Lactate Buildup at the Site of Chronic Inflammation Promotes Disease by Inducing CD4(+) T Cell Metabolic Rewiring. Cell Metab. 2019;30(6):1055–74 e8. [PubMed: 31708446]
18. Rochette L, Meloux A, Zeller M, Malka G, Cottin Y, Vergely C. Mitochondrial SLC25 Carriers: Novel Targets for Cancer Therapy. Molecules. 2020;25(10).
19. Pan Z, Choi S, Ouadid-Ahidouch H, Yang JM, Beattie JH, Korichneva I. Zinc transporters and dysregulated channels in cancers. Front Biosci (Landmark Ed). 2017;22:623–43. [PubMed: 27814637]
20. Gorbatenko A, Olesen CW, Boedtkjer E, Pedersen SF. Regulation and roles of bicarbonate transporters in cancer. Front Physiol. 2014;5:130. [PubMed: 24795638]
21. Gu HF. Genetic, Epigenetic and Biological Effects of Zinc Transporter (SLC30A8) in Type 1 and Type 2 Diabetes. Curr Diabetes Rev. 2017;13(2):132–40. [PubMed: 26593983]
22. VanWert AL, Gionfriddo MR, Sweet DH. Organic anion transporters: discovery, pharmacology, regulation and roles in pathophysiology. Biopharm Drug Dispos. 2010;31(1):1–71. [PubMed: 19953504]
23. Nemtsova MV, Zaletaev DV, Bure IV, Mikhaylenko DS, Kuznetsova EB, Alekseeva EA, et al. Epigenetic Changes in the Pathogenesis of Rheumatoid Arthritis. Front Genet. 2019;10:570. [PubMed: 31258550]
24. Doody KM, Bottini N, Firestein GS. Epigenetic alterations in rheumatoid arthritis fibroblast-like synoviocytes. Epigenomics. 2017;9(4):479–92. [PubMed: 28322585]
25. Ai R, Laragione T, Hammaker D, Boyle DL, Wildberg A, Maeshima K, et al. Comprehensive epigenetic landscape of rheumatoid arthritis fibroblast-like synoviocytes. Nat Commun. 2018;9(1):1921. [PubMed: 29765031]
26. Bustamante MF, Oliveira PG, Garcia-Carbonell R, Croft AP, Smith JM, Serrano RL, et al. Hexokinase 2 as a novel selective metabolic target for rheumatoid arthritis. Ann Rheum Dis. 2018;77(11):1636–43. [PubMed: 30061164]
27. Gosselin D, Skola D, Coufal NG, Holtman IR, Schlachetzki JCM, Sajti E, et al. An environment-dependent transcriptional network specifies human microglia identity. Science. 2017;356(6344).
28. Seidman JS, Troutman TD, Sakai M, Gola A, Spann NJ, Bennett H, et al. Niche-Specific Reprogramming of Epigenetic Landscapes Drives Myeloid Cell Diversity in Nonalcoholic Steatohepatitis. Immunity. 2020;52(6):1057–74 e7. [PubMed: 32362324]
29. Heinz S, Benner C, Spann N, Bertolino E, Lin YC, Laslo P, et al. Simple combinations of lineage-determining transcription factors prime cis-regulatory elements required for macrophage and B cell identities. Mol Cell. 2010;38(4):576–89. [PubMed: 20513432]
30. Liberzon A, Subramanian A, Pinchback R, Thorvaldsdottir H, Tamayo P, Mesirov JP. Molecular signatures database (MSigDB) 3.0. Bioinformatics. 2011;27(12):1739–40. [PubMed: 21546393]
31. Liberzon A, Birger C, Thorvaldsdottir H, Ghandi M, Mesirov JP, Tamayo P. The Molecular Signatures Database (MSigDB) hallmark gene set collection. Cell Syst. 2015;1(6):417–25. [PubMed: 26771021]
32. Subramanian A, Tamayo P, Mootha VK, Mukherjee S, Ebert BL, Gillette MA, et al. Gene set enrichment analysis: a knowledge-based approach for interpreting genome-wide expression profiles. Proc Natl Acad Sci U S A. 2005;102(43):15545–50. [PubMed: 16199517]

33. Beckonert O, Keun HC, Ebbels TM, Bundy J, Holmes E, Lindon JC, et al. Metabolic profiling, metabolomic and metabonomic procedures for NMR spectroscopy of urine, plasma, serum and tissue extracts. Nat Protoc. 2007;2(11):2692–703. [PubMed: 18007604]
34. Nagana Gowda GA, Raftery D. Analysis of Plasma, Serum, and Whole Blood Metabolites Using (1)H NMR Spectroscopy. Methods Mol Biol. 2019;2037:17–34. [PubMed: 31463837]
35. Tiziani S, Emwas AH, Lodi A, Ludwig C, Bunce CM, Viant MR, et al. Optimized metabolite extraction from blood serum for 1H nuclear magnetic resonance spectroscopy. Anal Biochem. 2008;377(1):16–23. [PubMed: 18312846]
36. Bartok B, Firestein GS. Fibroblast-like synoviocytes: key effector cells in rheumatoid arthritis. Immunol Rev. 2010;233(1):233–55. [PubMed: 20193003]
37. Rodriguez-Trillo A, Mosquera N, Pena C, Rivas-Tobio F, Mera-Varela A, Gonzalez A, et al. Non-Canonical WNT5A Signaling Through RYK Contributes to Aggressive Phenotype of the Rheumatoid Fibroblast-Like Synoviocytes. Front Immunol. 2020;11:555245. [PubMed: 33178184]
38. Garcia-Carbonell R, Divakaruni AS, Lodi A, Vicente-Suarez I, Saha A, Cheroutre H, et al. Critical Role of Glucose Metabolism in Rheumatoid Arthritis Fibroblast-like Synoviocytes. Arthritis Rheumatol. 2016;68(7):1614–26. [PubMed: 26815411]
39. Zou Y, Zeng S, Huang M, Qiu Q, Xiao Y, Shi M, et al. Inhibition of 6-phosphofructo-2-kinase suppresses fibroblast-like synoviocytes-mediated synovial inflammation and joint destruction in rheumatoid arthritis. Br J Pharmacol. 2017;174(9):893–908. [PubMed: 28239846]
40. Biniecka M, Canavan M, McGarry T, Gao W, McCormick J, Cregan S, et al. Dysregulated bioenergetics: a key regulator of joint inflammation. Ann Rheum Dis. 2016;75(12):2192–200. [PubMed: 27013493]
41. Tolboom TC, Pieterman E, van der Laan WH, Toes RE, Huidekoper AL, Nelissen RG, et al. Invasive properties of fibroblast-like synoviocytes: correlation with growth characteristics and expression of MMP-1, MMP-3, and MMP-10. Ann Rheum Dis. 2002;61(11):975–80. [PubMed: 12379519]
42. Qadri M, Jay GD, Zhang LX, Richendrfer H, Schmidt TA, Elsaid KA. Proteoglycan-4 regulates fibroblast to myofibroblast transition and expression of fibrotic genes in the synovium. Arthritis Res Ther. 2020;22(1):113. [PubMed: 32404156]
43. You S, Yoo SA, Choi S, Kim JY, Park SJ, Ji JD, et al. Identification of key regulators for the migration and invasion of rheumatoid synoviocytes through a systems approach. Proc Natl Acad Sci U S A. 2014;111(1):550–5. [PubMed: 24374632]
44. McInnes IB, Buckley CD, Isaacs JD. Cytokines in rheumatoid arthritis - shaping the immunological landscape. Nat Rev Rheumatol. 2016;12(1):63–8. [PubMed: 26656659]
45. Han D, Fang Y, Tan X, Jiang H, Gong X, Wang X, et al. The emerging role of fibroblast-like synoviocytes-mediated synovitis in osteoarthritis: An update. J Cell Mol Med. 2020;24(17):9518–32. [PubMed: 32686306]
46. Song G, Lu Q, Fan H, Zhang X, Ge L, Tian R, et al. Inhibition of hexokinases holds potential as treatment strategy for rheumatoid arthritis. Arthritis Res Ther. 2019;21(1):87. [PubMed: 30944034]
47. Bott AJ, Peng IC, Fan Y, Faubert B, Zhao L, Li J, et al. Oncogenic Myc Induces Expression of Glutamine Synthetase through Promoter Demethylation. Cell Metab. 2015;22(6):1068–77. [PubMed: 26603296]
48. Takahashi S, Saegusa J, Sendo S, Okano T, Akashi K, Irino Y, et al. Glutaminase 1 plays a key role in the cell growth of fibroblast-like synoviocytes in rheumatoid arthritis. Arthritis Res Ther. 2017;19(1):76. [PubMed: 28399896]
49. Li T, Le A. Glutamine Metabolism in Cancer. Adv Exp Med Biol. 2018;1063:13–32. [PubMed: 29946773]
50. Altman BJ, Stine ZE, Dang CV. From Krebs to clinic: glutamine metabolism to cancer therapy. Nat Rev Cancer. 2016;16(10):619–34. [PubMed: 27492215]
51. Guma M, Sanchez-Lopez E, Lodi A, Garcia-Carbonell R, Tiziani S, Karin M, et al. Choline kinase inhibition in rheumatoid arthritis. Ann Rheum Dis. 2015;74(7):1399–407. [PubMed: 25274633]

52. Bonaventura P, Lamboux A, Albarede F, Miossec P. A Feedback Loop between Inflammation and Zn Uptake. PLoS One. 2016;11(2):e0147146. [PubMed: 26845700]

53. Zhang J, Visser F, King KM, Baldwin SA, Young JD, Cass CE. The role of nucleoside transporters in cancer chemotherapy with nucleoside drugs. Cancer Metastasis Rev. 2007;26(1):85–110. [PubMed: 17345146]

54. Miller DM, Thomas SD, Islam A, Muench D, Sedoris K. c-Myc and cancer metabolism. Clin Cancer Res. 2012;18(20):5546–53. [PubMed: 23071356]

55. Song W, Li D, Tao L, Luo Q, Chen L. Solute carrier transporters: the metabolic gatekeepers of immune cells. Acta Pharm Sin B. 2020;10(1):61–78. [PubMed: 31993307]

56. Pap T, Nawrath M, Heinrich J, Bosse M, Baier A, Hummel KM, et al. Cooperation of Ras- and c-Myc-dependent pathways in regulating the growth and invasiveness of synovial fibroblasts in rheumatoid arthritis. Arthritis Rheum. 2004;50(9):2794–802. [PubMed: 15457447]

57. Richart L, Carrillo-de Santa Pau E, Rio-Machin A, de Andres MP, Cigudosa JC, Lobo VJS, et al. BPTF is required for c-MYC transcriptional activity and in vivo tumorigenesis. Nat Commun. 2016;7:10153. [PubMed: 26729287]

58. Chen H, Liu H, Qing G. Targeting oncogenic Myc as a strategy for cancer treatment. Signal Transduct Target Ther. 2018;3:5. [PubMed: 29527331]

A

Occurrence	pathway
6	PI3K-Akt signaling pathway
5	Metabolism of carbohydrates
5	Integration of energy metabolism
4	SLC-mediated transmembrane transport
4	Transport of small molecules
4	Transport of inorganic cations/anions and a mino acids/oligopeptides
4	Amino Acid metabolism
4	Pyruvate metabolism
4	Sphingolipid signaling pathway
4	Prostaglandin Synthesis and Regulation
4	LPA receptor mediated events
4	LPA4-mediated signaling events
4	HIF-1-alpha transcription factor network
4	Glycolysis and Gluconeogenesis
4	Ceramide signaling pathway
3	Valine Leucine Isoleucine degradation
3	Serine biosynthesis
3	Propanoate metabolism
3	NAD metabolism, sirtuins and aging
3	Metabolism
3	Cholesterol metabolism

B

	pathway	q value
RNA-seq	Amino acid and oligopeptide SLC transporter s	0.040
	Pancreatic secretion	0.040
	Synthesis of bile acids and bile salts via 27-h ydroxycholesterol	0.040
	Transport of inorganic cations/anions and am ino acids/oligopeptides	0.040
	ABC transporters	0.050
	Prostaglandin Synthesis and Regulation	0.050
	Transport of small molecules	0.050
	Amino acid transport across the plasma mem brane	0.040
ATAC-seq	Transport of small molecules	0.000
	PI3K-Akt Signaling Pathway	0.000
	Prostaglandin Synthesis and Regulation	0.000
	PIP3 activates AKT signaling	0.001
	Amino Acid metabolism	0.001
	SLC-mediated transmembrane transport	0.002
	LPA receptor mediated events	0.003
	Sphingolipid signaling pathway	0.004
	Metabolism of carbohydrates	0.006
	Metabolism of lipids	0.009
	Choline metabolism in cancer	0.012
	Ceramide signaling pathway	0.037
	NAD metabolism, sirtuins and aging	0.038
	Arginine Proline metabolism	0.044
	HIF-1-alpha transcription factor network	0.047
H3K4me1	LPA receptor mediated events	0.001
	Nicotinate Nicotinamide metabolism	0.004
	Glycolysis / Gluconeogenesis	0.013
	HIF-1-alpha transcription factor network	0.016
	PI3K-Akt Signaling Pathway	0.022
	Metabolism of carbohydrates	0.027
	Transport of inorganic cations/anions and am ino acids/oligopeptides	0.028
H3K4me3	Sterol Regulatory Element-Binding Proteins (SREBP) signalling	0.000
	Regulation of cholesterol biosynthesis by SRE BP (SREBF)	0.000
	Cholesterol biosynthesis, regulation and trans port	0.001
	superpathway of cholesterol biosynthesis	0.002
	Cholesterol biosynthesis	0.002
	Cholesterol Biosynthesis Pathway	0.003
	PI3K-Akt signaling pathway	0.003
	Metabolic reprogramming in colon cancer	0.004
	SREBF and miR33 in cholesterol and lipid ho meostasis	0.004
	PI3K-Akt Signaling Pathway	0.006
	HIF-1-alpha transcription factor network	0.007
	Metabolism of proteins	0.024
	LPA receptor mediated events	0.031
	Cysteine Metabolism	0.034
	Inositol phosphate metabolism	0.039
	Amino Acid metabolism	0.048
H3K27ac	Metabolism of carbohydrates	0.000
	HIF-1-alpha transcription factor network	0.000
	Metabolism	0.000
	PI3K-Akt signaling pathway	0.002
	Amino Acid metabolism	0.005
	Aminosugars metabolism	0.005
	Energy Metabolism	0.005
	Glycolysis / Gluconeogenesis	0.008
	HIF-1 signaling pathway	0.008
	Urea cycle and metabolism of arginine, prolin e, glutamate, aspartate and asparagine	0.013
	Transport of inorganic cations/anions and am ino acids/oligopeptides	0.013
	Prostaglandin Synthesis and Regulation	0.017
	Amino acid transport across the plasma mem brane	0.022
	mTOR signaling pathway	0.023
	LPA4-mediated signaling events	0.023
	Glycolysis and Gluconeogenesis	0.025
	Cholesterol biosynthesis I	0.036
	Cholesterol biosynthesis II (via 24,25-dihydro lanosterol)	0.036
	Cholesterol biosynthesis III (via desmosterol)	0.036
	Cholesterol Biosynthesis Pathway	0.039
	Nicotinate Nicotinamide metabolism	0.039
	Phosphatidylinositol Phosphate Metabolism	0.039
	Metabolism of vitamins and cofactors	0.045
	Valine Leucine Isoleucine degradation	0.048
	Phosphatidylinositol phosphate metabolism	0.048
	PIP3 activates AKT signaling	0.045

Figure 1. Unsupervised analysis of metabolic pathways associated with differentially modified genome-wide chromatin and DNA states and gene expression between OA and RA FLS.

A. Metabolic-related pathways and their occurrences in RA FLS. **B.** Metabolic pathways per histone modification, WGBS, ATAC-Seq and RNA-Seq.

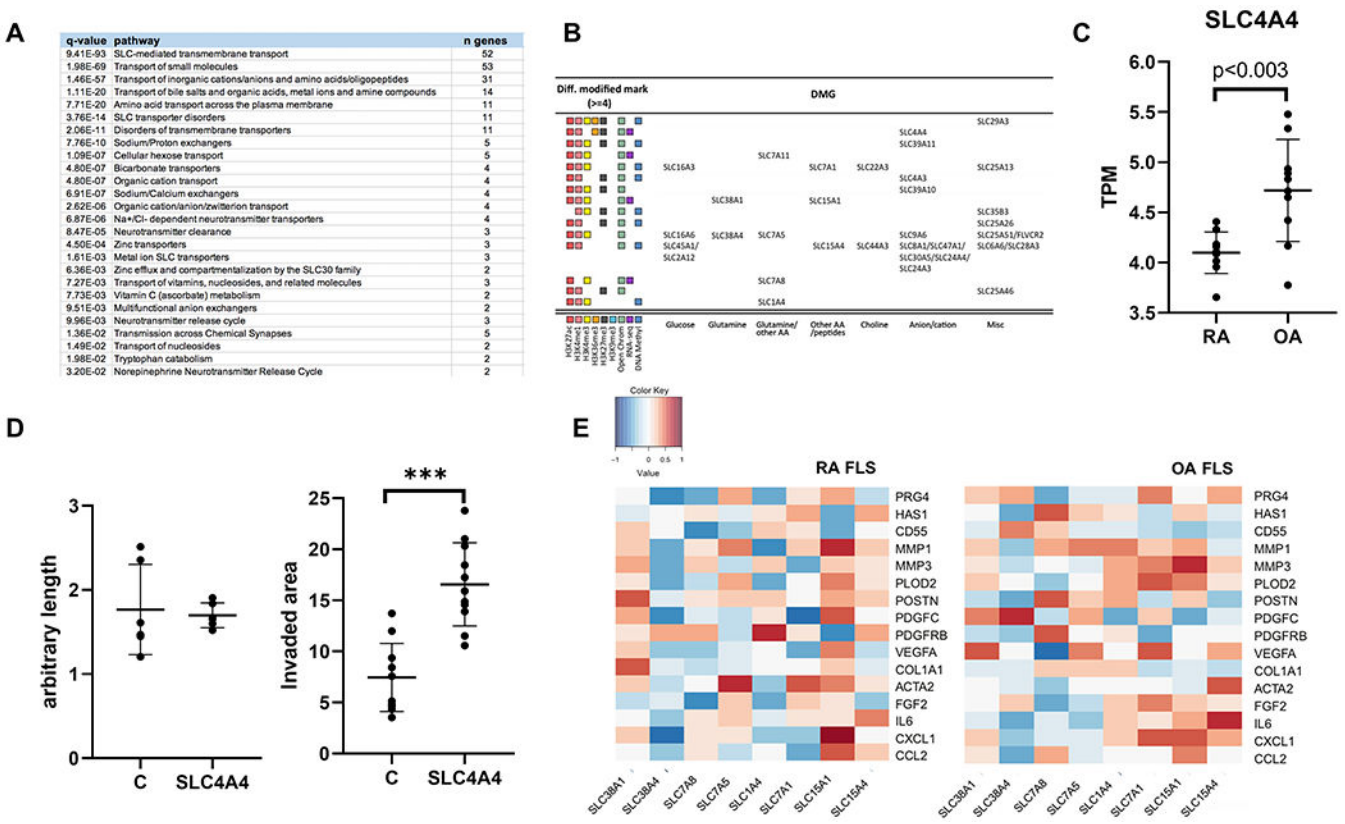

Figure 2. Supervised analysis of SLC-mediated transmembrane transporters showed differential marking between OA and RA FLS.

A. Pathway analysis using Reactome with the 78 genes associated with differentially modifications in at least 3 genome-wide chromatin and DNA states between OA and RA FLS to identify the existence of predominant nutrient transporters. **B.** Number and type of dynamic chromatin changes for each of the listed histone post-translational modifications, ATAC-Seq, RNA-Seq and WGBS signal between OA and RA FLS in the 32 genes associated with differentially modifications in at least 4 genome-wide chromatin and DNA states. **C.** Expression of *SLC4A4* by RNAseq in TPM (transcripts per million). **D.** RA were transfected with SLC4A4 siRNA as described in methods and cells were scratched for migration **(left)** or plated in matrigel for invasion **(right)** and given media with glucose and glutamine. Results are an average of 3 cell lines graphed with standard deviation. *P*-values were obtained by using two-tailed t test. **E.** Heat map to show the association in gene expression between amino acid related SLC transporters and genes related to FLS aggressive behavior in 10 RA and 10 OA FLS. Color key above heat map shows Pearson's correlation coefficients. * denotes p<0.05

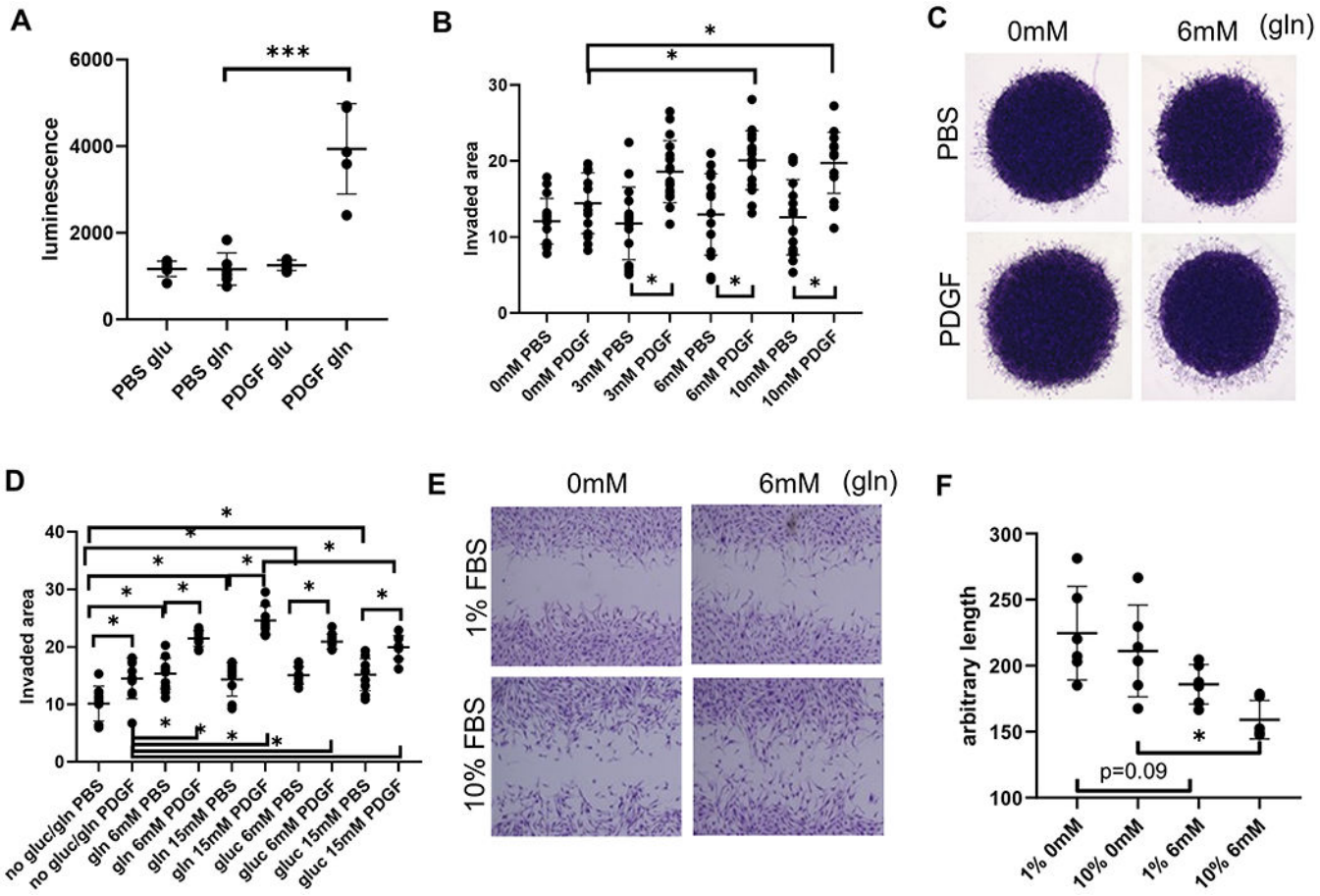

Figure 3. Glutamine availability enhances invasion and migration of RA FLS.

A. Quantification of luminescence of RA FLS to measure intracellular glutamine (gln) and glutamate (glu) levels after removal of glucose and 2-hour PDGF stimulation. **B-C.** RA FLS were starved overnight without glucose and then starved of glutamine for 4 hours. RA FLS were plated for invasion as described in methods. RA FLS were stimulated with various amounts of glutamine with or without PDGF stimulation. **B.** Quantification and **C**. Representative images of RA FLS invasion. **D.** RA FLS were plated for invasion as described in methods and stimulated with various amounts of either glucose (gluc) or glutamine with or without PDGF stimulation. Quantification of invaded area is shown. **E-F.** RA FLS were plated, starved overnight in media with 0.1% FBS and scratched. Media without glucose was added along with various concentrations of glutamine and allowed to migrate in 1% or 10% dialyzed FBS. **E.** Representative images of RA FLS migration. **F.** Quantification of migration as detailed in methods. **(A-F)** Results are average of 3-4 FLS cell lines. Averages were graphed with standard deviation. *P*-values were obtained by using one-way ANOVA followed by Tukey's multiple comparisons test.

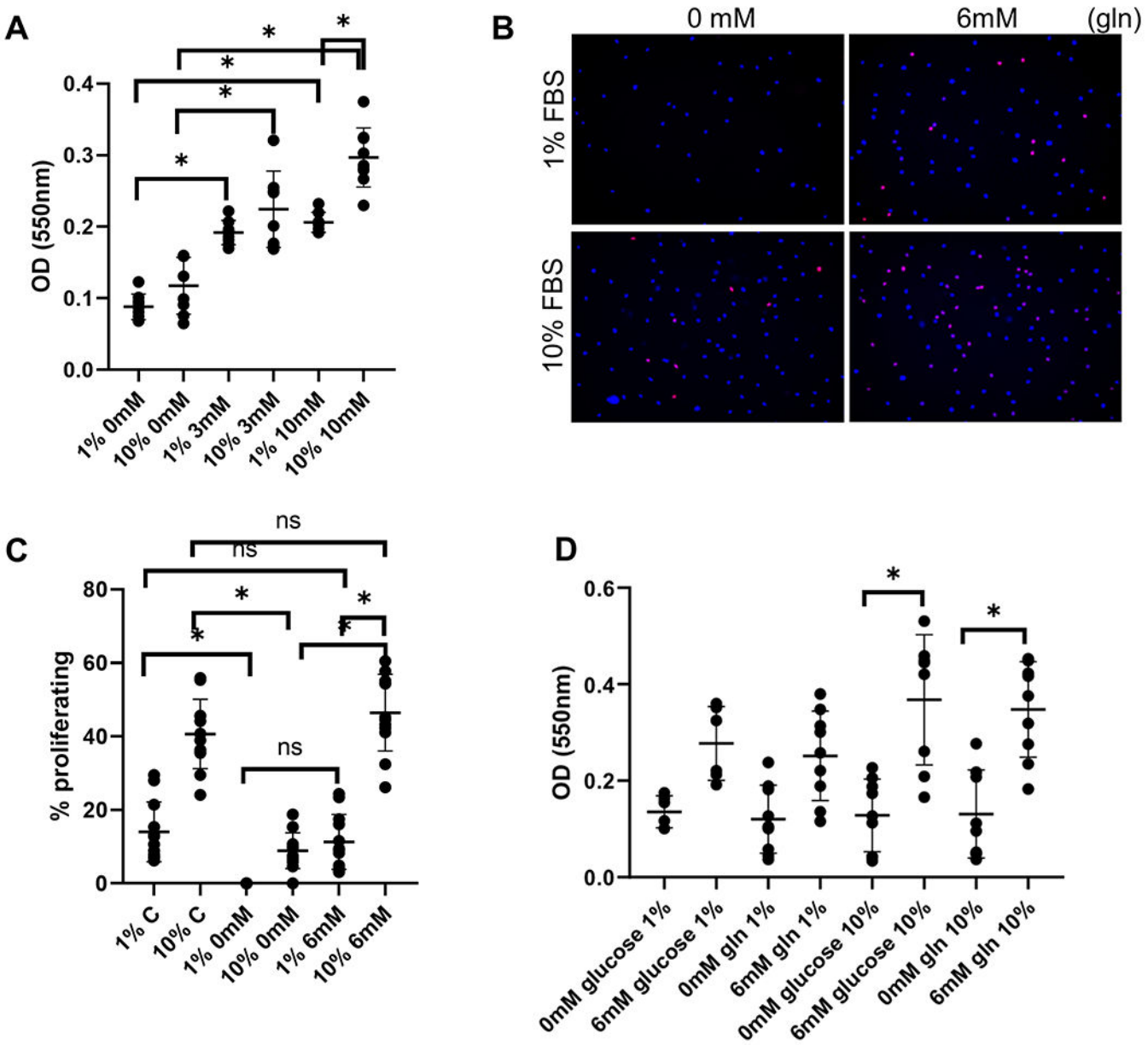

Figure 4. Glutamine availability enhances proliferation of RA FLS.

A. RA FLS were plated as explained in methods, starved overnight with 0.1% FBS media, and stimulated with various amounts of glutamine without glucose. MTT was added after 4 days of stimulation. **B-C**. FLS were starved overnight with media containing 0.1% FBS without glucose and different concentrations of glutamine, and left to proliferate for 4 days. Representative images are displayed in figure **B** for 0 mM and 6 mM glutamine in 1% or 10% dialyzed FBS with Hoechst (blue) and EdU staining. **C.** Quantification of EdU positive cells divided by number Hoechst positive cells where control (C) is DMEM with 25mM glucose and 6mM of glutamine. **D.** Quantification of optical density from 7-day MTT of FLS stimulated with either glucose or glutamine in 1% FBS or 10% FBS. Results are an

average of 3 FLS cell lines graphed with standard deviation. *P*-values were obtained by one-way ANOVA followed by Tukey's multiple comparisons test.

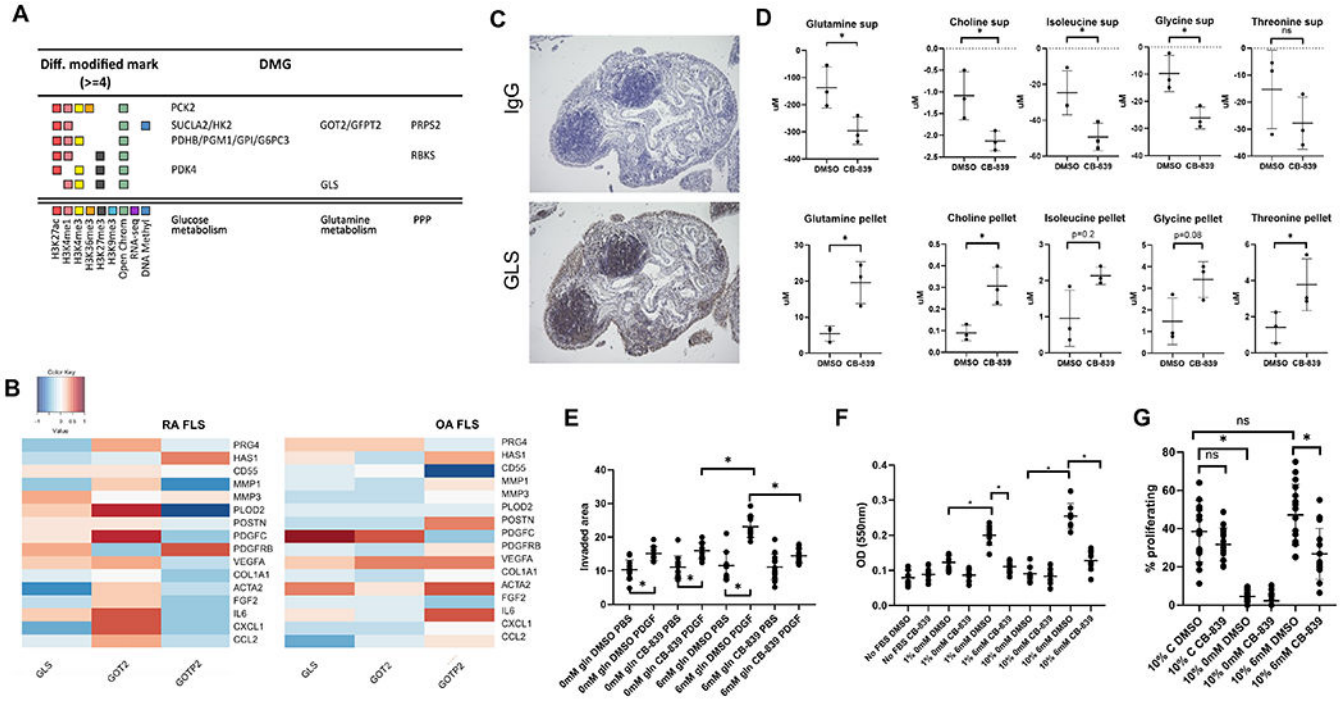

Figure 5. Effect of GLS inhibition in FLS invasion and proliferation.

Number and type of dynamic chromatin changes of genes with a change in at least 4 marks between OA and RA FLS. **B.** Heat map to show the association between glutamine related genes and genes related to FLS aggressive behavior in in 10 RA and 10 OA FLS. Color key above heat map shows Pearson's correlation coefficients. **C.** Distribution of GLS expression in RA synovial tissue. **D.** 1D ^{1}H-NMR spectrum and concentration (μM) of glutamine in pellet and supernatant (sup) in 3 RA FLS after 4-hours PDGF stimulation with and without CB-839 (10uM). *P*-values were obtained by two-tailed t- test. **E.** RA FLS were plated for invasion and deprived of glucose and given glutamine with and without CB-839. Quantification is shown. **F.** Quantification from 4-day MTT assay of RA FLS deprived of glucose in the indicated conditions. **G.** EdU proliferation of RA FLS with and without CB-839 as percentage of EdU expressing cells over total number of cells. Control (C) is DMEM with 25mM glucose and 6mM of glutamine. **(E-G)**. Results are an average of 4 RA cell lines graphed with standard deviation. *P*-values were obtained by one-way ANOVA.

A

Motif Name	Log 10 (P)	% of Target Seq with Motifs	% of Backg Seq. with Motifs
c-Myc	-8	47.29%	35.36%
Tlx?	-7.63	37.44%	26.60%
USF1	-7.25	39.90%	29.18%
n-Myc	-6.47	52.22%	41.64%
RORa	-6.43	14.29%	7.95%
Sox3	-5.54	76.85%	68.09%
Max	-5.49	45.81%	36.51%
GATA:SCL	-5.39	12.32%	7.01%
Mef2c	-5.27	32.51%	24.31%
TEAD2	-5.04	38.92%	30.47%
RORg	-4.78	9.85%	5.46%
MNT	-4.74	56.65%	48.05%
NPAS	-4.62	73.89%	66.01%

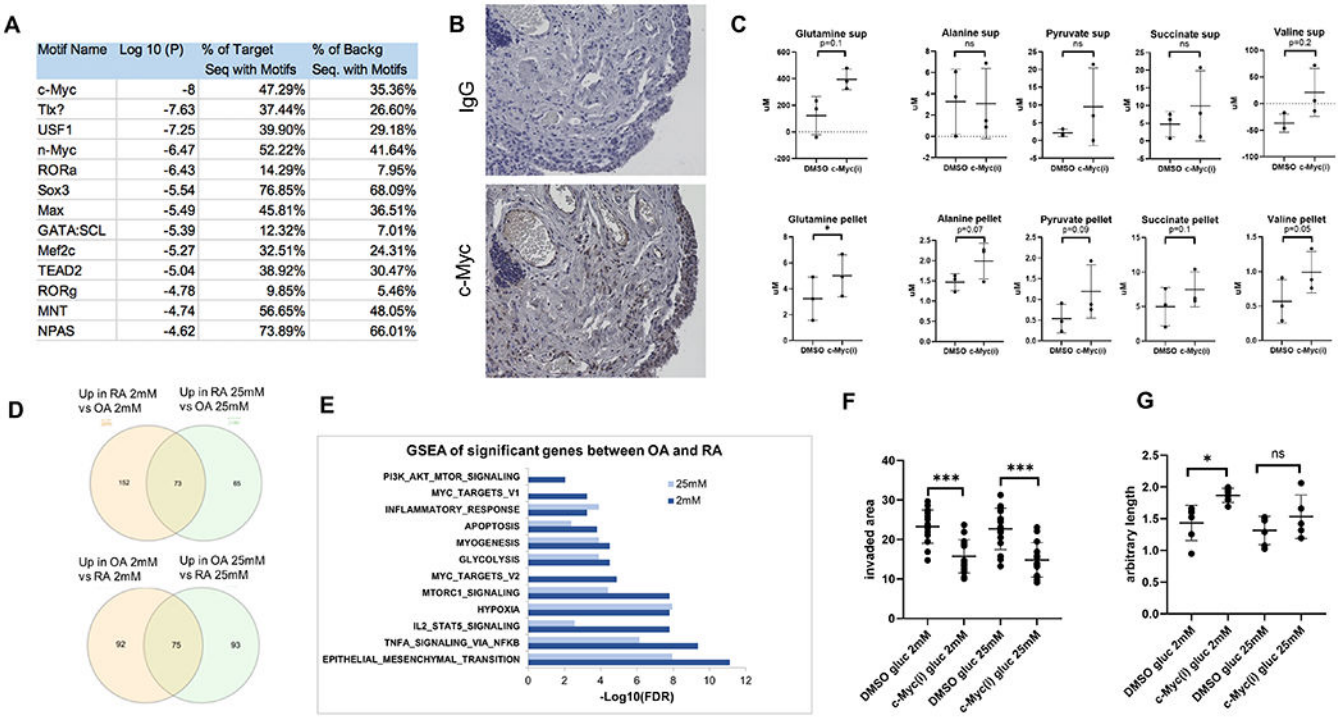

Figure 6. Effect of c-Myc inhibition on FLS invasion and proliferation.

A. Motif analysis of the promoter of genes associated with altered in at least four genome-wide states. **B.** Distribution of c-Myc expression in RA synovial tissue. **C.** Concentration (μM) of metabolites in pellet and supernatant obtained from 1D ^{1}H- NMR spectrum using 3 RA cell lines in 1% dialyzed media with 6mM glutamine with or without c-Myc inhibitor (10uM) for 24 hours. **D.** Venn Diagram of significantly upregulated genes in 4 RA compared to 3 OA FLS cell lines in 25mM and 2mM (top) and of significantly upregulated genes in OA compared to RA in 25mM and 2mM (bottom). **E.** Gene set enrichment analysis (GSEA) using Hallmark gene sets differentially expressed between RA FLS and OA FLS in 25 mM or 2 mM glucose. **F-G.** RA FLS were plated for invasion or migration as described in methods in 1% dialyzed media with 6mM glutamine and either 2mM glucose or 25mM glucose, and with or without c-Myc inhibitor (i: 10uM). Results are an average of 3 cell lines with standard deviation. *P*-values were obtained by one-way ANOVA followed by Tukey's multiple comparisons test.